Check for updates

NEUROSCIENCE

Presynaptic Ube3a E3 ligase promotes synapse elimination through down-regulation of BMP signaling

Kotaro Furusawa[1], Kenichi Ishii[1], Masato Tsuji[1], Nagomi Tokumitsu[1], Eri Hasegawa[1], Kazuo Emoto[1,2]*

Inactivation of the ubiquitin ligase Ube3a causes the developmental disorder Angelman syndrome, whereas increased Ube3a dosage is associated with autism spectrum disorders. Despite the enriched localization of Ube3a in the axon terminals including presynapses, little is known about the presynaptic function of Ube3a and mechanisms underlying its presynaptic localization. We show that developmental synapse elimination requires presynaptic Ube3a activity in *Drosophila* neurons. We further identified the domain of Ube3a that is required for its interaction with the kinesin motor. Angelman syndrome–associated missense mutations in the interaction domain attenuate presynaptic targeting of Ube3a and prevent synapse elimination. Conversely, increased Ube3a activity in presynapses leads to precocious synapse elimination and impairs synaptic transmission. Our findings reveal the physiological role of Ube3a and suggest potential pathogenic mechanisms associated with Ube3a dysregulation.

Angelman syndrome is a developmental disorder characterized by intellectual disability, motor dysfunction, epilepsy, and absence of speech (*1*, *2*). Genetic studies have identified the evolutionarily conserved E3 ubiquitin ligase Ube3a as the causal factor in Angelman syndrome. Loss of functional Ube3a impairs developmental synapse plasticity (*3*–*6*). Conversely, increased Ube3a dosage because of the copy number variations within the *Ube3a* locus leads to autism spectrum disorders (ASDs), which is often associated with impaired synaptic transmission (*7*, *8*). To understand how Ube3a regulates synapse plasticity and function, previous studies have focused primarily on the postsynaptic function of Ube3a (*9*–*11*). However, immunochemical and electron microscopic studies have shown that Ube3a protein in human and mouse cortical neurons is predominantly localized in axon terminals including presynapses, rather than postsynapses and dendrites (*12*–*14*). Compared with the accumulated evidence supporting the role in spine development and postsynaptic plasticity, little is known about presynaptic functions of Ube3a, including whether dysregulation of presynaptic Ube3a contributes to synaptic defects in Angelman syndrome and ASDs.

Drosophila C4da neurons undergo presynapse elimination during metamorphosis

Drosophila class IV dendrite arborization (C4da) sensory neurons innervate dendritic branches over the body wall while projecting axons to the ventral nerve cord (VNC) to form synaptic contacts with second-order neurons (Fig. 1A and fig. S1) (*15*–*17*). C4da neurons have been used to study molecular mechanisms of dendrite remodeling because they undergo dendrite pruning in the first 24 hours after puparium formation (APF) followed by regeneration of adult-specific dendritic arbors in the later pupal stage (*18*–*22*). We show that C4da neurons remodel presynapses as well as dendrites during metamorphosis. To visualize presynapses and axonal-dendritic branches simultaneously in C4da neurons, we expressed the presynaptic marker Bruchpilot (Brp)::mCherry and mCD8GFP in C4da neurons using the GAL4–upstream activator sequence (UAS) system (*23*). Consistent with previous studies (*24*, *25*), Brp::mCherry clearly labeled punctate structures on C4da axon terminals in third instar larvae (Fig. 1B and movie S1), which allowed us to quantify presynapse numbers on C4da axonal terminals. We consistently observed ~400 Brp::mCherry-positive spots in each of the abdominal segment A3 to A5 during wandering larvae and white pupa stages (Fig. 1B). After initiating metamorphosis, however, the number of the Brp::mCherry-positive spots was progressively reduced until 24 hours APF, at which time Brp::mCherry signal was absent from C4da axon terminals, indicating that presynapses in C4da neurons are removed during early metamorphosis (Fig. 1B and movie S2). This presynapse elimination was consistently observed in all segments in 24 hours APF (fig. S2, A and B). Single-cell analyses revealed a progressive loss of presynapses on the contralateral axon branches with concomitant retraction of axon terminals (fig. S3). In adult flies, Brp::mCherry-positive dots were visible on C4da axon terminals, suggesting that C4da neurons regenerate adult-specific synapse connectivity during the late pupal stage (fig. S4). It is thus likely that C4da neurons remodel both presynapses and dendrites in a comparable time window during metamorphosis (Fig. 1C and fig. S4).

Ube3a E3 ligase is required for presynapse elimination

Previous studies identified multiple molecules required for dendrite pruning in C4da neurons, including ecdysone signaling molecules, ubiquitin-proteasome system-related molecules, cytoskeletal regulators, and calcium signaling molecules (*26*–*32*). We thus examined whether dendrite pruning and presynapse elimination are mediated by a common molecular mechanism. We first confirmed that the ecdysone signaling pathway triggers presynapse elimination; a dominant-negative version of the ecdysone receptor EcR or RNA interference (RNAi) suppression of the EcR transcriptional target Sox14 impaired presynapse elimination as well as dendrite pruning in C4da neurons (fig. S5). We next tested the components involved in local degradation of dendritic branches and found that only the E1 ubiquitin-activating enzyme Uba1 was required for both presynapse elimination and dendrite pruning (Fig. 2, A and B, and figs. S6 and S7). Because Uba1 acts with Cullin1 E3 ligase in dendrite pruning (*32*), we next performed RNAi suppression of *Cullin1* in C4da neurons and found that Cullin1 is dispensable for synapse elimination (Fig. 2, A and B, and fig. S7), suggesting that distinct E3 ligases might function in dendrite pruning and synapse elimination. We thus performed an RNAi screen for E3 ligases involved in presynapse elimination, focusing on genes that are expressed in the nervous system according to the FlyBase information (https://flybase.org/reports/FBgg0000069). We found that C4da-specific suppression of *Ube3a* caused severe presynapse elimination defects without affecting dendrite pruning (Fig. 2, A and B; fig. S7; and table S1). Similar presynapse elimination defects were observed with two independent *Ube3a* null alleles (Fig. 2, C and D). Furthermore, C4da neuron–specific expression of wild-type Ube3a, but not a catalytically inactive Ube3a (Ube3a C941A), completely rescued synapse elimination defects in *Ube3a* mutants (Fig. 2, C and D), confirming that Ube3a E3 ligase acts cell-autonomously in C4da neurons to promote presynapse elimination (Fig. 2E).

Ube3a is transported to presynapses in a kinesin motor–dependent manner

How could Ube3a function specifically in presynapse elimination without affecting dendrite pruning? One potential scenario might be localized function of Ube3a in C4da presynapses on the axon terminals. To test this model, we assessed subcellular localization of an epitope-tagged version of Ube3a (Ube3a-Flag) expressed in *Ube3a*-null C4da neurons. Because Ube3a-Flag completely rescued the presynapse elimination defects in *Ube3a* C4da neurons (Fig. 2, C and D), we reasoned that it likely mimics localization of endogenous Ube3a proteins in C4da neurons. We found that Ube3a-Flag was predominantly localized in presynapses on C4da axon terminals, whereas no obvious expression was observed in dendrites (Fig. 3, A

[1]Department of Biological Sciences, Graduate School of Science, The University of Tokyo, 7-3-1 Hongo, Bunkyo-ku, Tokyo 113-0033, Japan. [2]International Research Center for Neurointelligence (WPI-IRCN), The University of Tokyo, 7-3-1 Hongo, Bunkyo-ku, Tokyo 113-0033, Japan.
*Corresponding author. Email: emoto@bs.s.u-tokyo.ac.jp

Downloaded from https://www.science.org at University Van Amsterdam on April 13, 2025

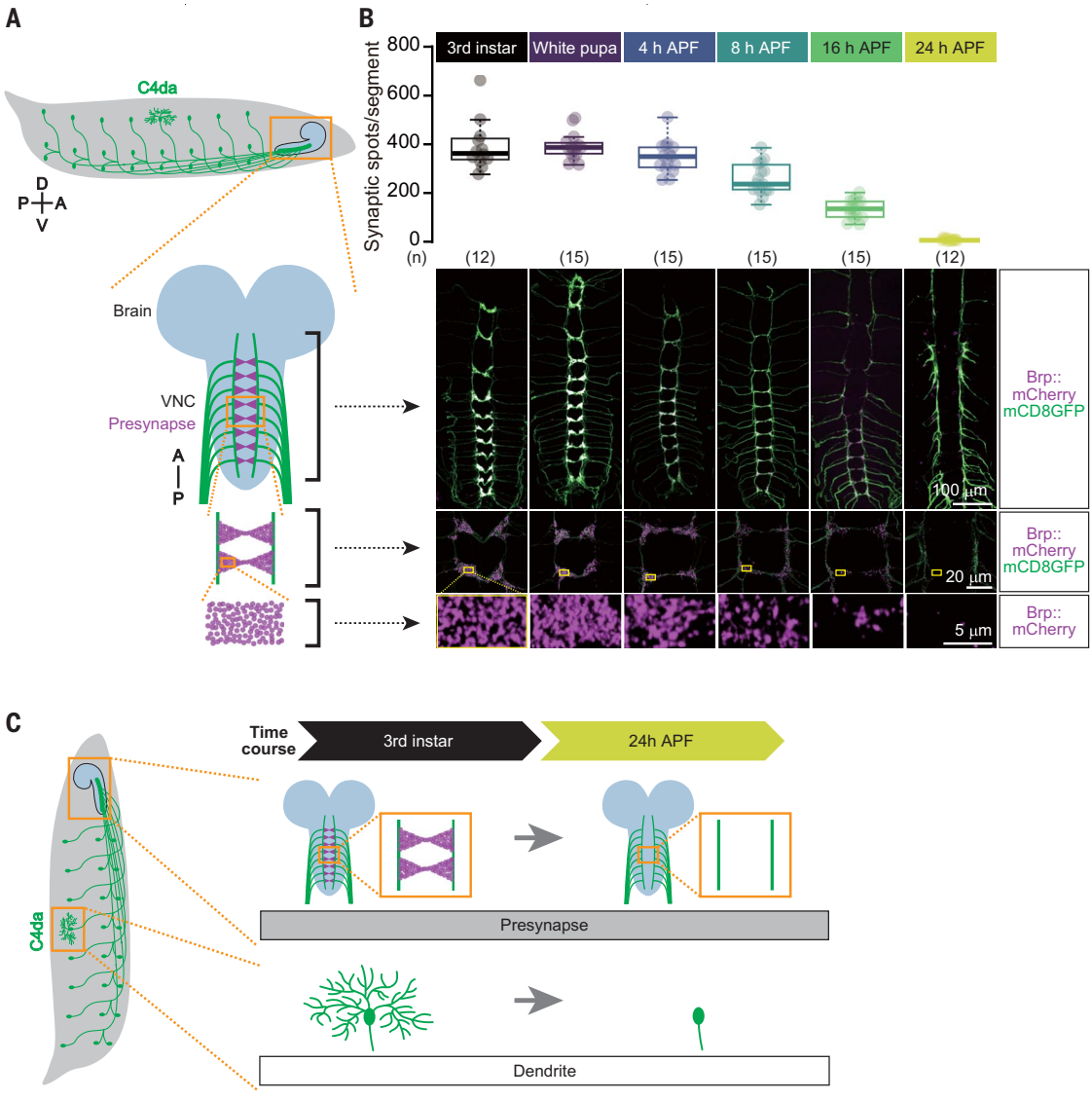

Fig. 1. *Drosophila* C4da neurons undergo presynapse elimination during metamorphosis. (**A**) A schematic view of dendrite arborizations and axonal projections of C4da neurons in third instar larvae. (Bottom) Axon terminal projections (green) and presynapses (magenta) in the ventral nerve cord (VNC). (**B**) The number of presynaptic marker puncta in the abdominal segments of C4da neurons from third instar larval stage to 24 hours APF. Box plots indicate the median, 25th and 75th percentiles, the data range except for outliers, and outliers. (Bottom) Presynapses (magenta) and axon terminals (green) of C4da neurons. (**C**) A schematic view of presynapse elimination and dendrite pruning in C4da neurons during metamorphosis.

and B). Live-imaging of Ube3a::GFP (green fluorescent protein) in C4da axons revealed anterograde transports of Ube3a from the soma to axon terminals with a constant speed (Fig. 3, C to F, and movie S3). This transport speed (483.8 nm/s on average) (Fig. 3F) was within the range of kinesin motor-mediated axon transport (*33*). Indeed, RNAi suppression of *kinesin heavy chain* (*khc*) in C4da neurons impaired presynapse localization of Ube3a (Fig. 3G). Consistently, C4da neurons with *khc* suppression showed severe presynapse elimination defects at 24 hours APF (Fig. 3H). Thus, Ube3a is transported to C4da presynapses through a kinesin motor–dependent mechanism (Fig. 3I).

Angelman syndrome–associated mutations attenuate axonal transport and presynapse localization of Ube3a

Ube3a protein is composed of multiple functional domains including an AZUL (N-terminal zinc-binding) domain at the N terminus and a HECT (homologous to the E6-AP carboxyl terminus) domain at the C terminus (Fig. 4A and fig. S8) (*1*, *2*). To date, the domain responsible for presynaptic targeting has been unknown. To identify such a domain, we constructed multiple mutant Ube3a::GFP that lack different domains and found that deletion of the middle domain containing tandem polar residues (TPRs) completely suppressed Ube3a localization to C4da presynapses, whereas deletion of AZUL or HECT showed less pronounced effects on Ube3a localization in presynapes (Fig. 4B). We found that an Angelman syndrome–linked missense mutation within the middle domain is conserved in *Drosophila* Ube3a (Fig. 4A and fig. S8) and that the same missense mutation D313V significantly interfered with Ube3a::GFP presynapse localizations (Fig. 4B). Because no significant difference was observed in expression levels between wild-type and mutated Ube3a in the soma (Fig. 4C), D313V likely affects presynaptic localization of Ube3a rather than expression levels and/or stability of Ube3a proteins. In addition to D313V, disease-associated mutations in evolutionarily conserved residues adjacent to the middle domain, V216G and I213T, also attenuated Ube3a::GFP localizations in presynapses (fig. S9). Given that Ube3a is transported to presynapses through a kinesin motor–dependent mechanism, we reasoned that these Angelman syndrome–associated mutations in the middle domain might affect interaction of Ube3a with the kinesin motor complex. To test this possibility, we monitored colocalization of Khc::GFP and Ube3a-Flag in C4da axons and found that D313V mutation strongly attenuated colocalization between Khc::GFP and Ube3a-Flag (Fig. 4, D and E). Furthermore, expression of Ube3a::GFP with D313V mutation or Ube3a::GFP lacking the middle region failed to rescue the presynapse elimination defects in *ube3a*-null C4da neurons (Fig. 4F). Similarly, genetic rescue experiments revealed

Downloaded from https://www.science.org at University Van Amsterdam on April 13, 2025

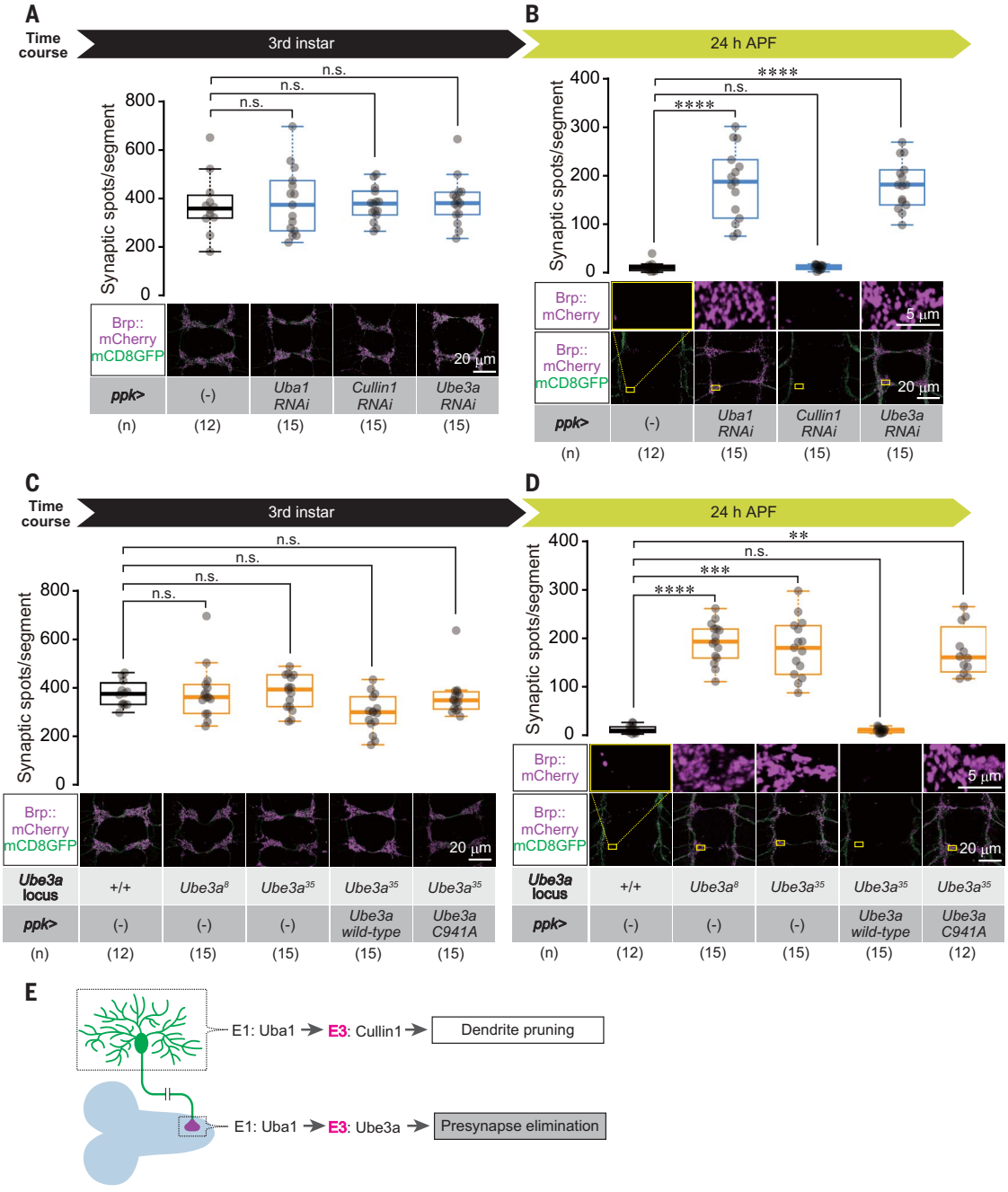

Fig. 2. Ube3a E3 ligase is required for presynapse elimination in C4da neurons. (**A** to **D**) Quantifications of the number of presynaptic marker puncta in an abdominal segment of C4da neurons at [(A) and (C)] third instar larval stage or [(B) and (D)] 24 hours APF. Box plots indicate the median, 25th and 75th percentiles, the data range except for outliers, and outliers. ****$P < 0.0001$, ***$P < 0.001$, **$P < 0.01$, n.s. $P \geq 0.05$, Kruskal-Wallis test with Dunn's multiple comparisons test. (Bottom) Presynapses in the abdominal segments. *ppk*, pickpocket. (**E**) Distinct E3 ligases, Ube3a and Cullin1, act in presynapse elimination and dendrite pruning, respectively.

that I213T and V216G mutations significantly affect Ube3a functions in synapse elimination as well as presynaptic localization of Ube3a in C4da neurons (fig. S9). Taken together, these data indicate that presynaptic localization of Ube3a is essential for its functions in presynapse elimination and suggest that the missense mutations and deletions that affect Ube3a presynaptic localization might impair synapse plasticity and contribute to Angelman syndrome. [Single-letter abbreviations for the amino acid residues are as follows: A, Ala; C, Cys; D, Asp; G, Gly; I, Ile; T, Thr; and V, Val. In the mutants, other amino acids were substituted at certain locations; for example, D313V indicates that aspartate at position 313 was replaced by valine.]

Ube3a down-regulates synaptic BMP signaling for synapse elimination

Because Ube3a-mediated presynapse elimination requires its E3 ligase activity (Fig. 2, C and D), Ube3a likely targets presynaptic proteins for proteosome-dependent degradation. Previous studies reported multiple Ube3a ligase targets, which differed according to cellular contexts as well as organisms (*2*, *34*, *35*). As a first step to determine the functionally relevant targets of Ube3a in presynapse elimination, we used gain-of-function approaches, reasoning that overexpression of bona fide Ube3a targets in a wild-type background should phenocopy the loss of *Ube3a* function. Among the potential Ube3a targets in neurons, overexpression of the bone morphogenetic protein (BMP) receptor Thickvein (Tkv) in C4da neurons caused severe synapse elimination defects comparable with those observed in *Ube3a* mutant neurons (table S2). The synapse elimination defects were further exacerbated by overexpressing a constitutive active version of

Downloaded from https://www.science.org at University Van Amsterdam on April 13, 2025

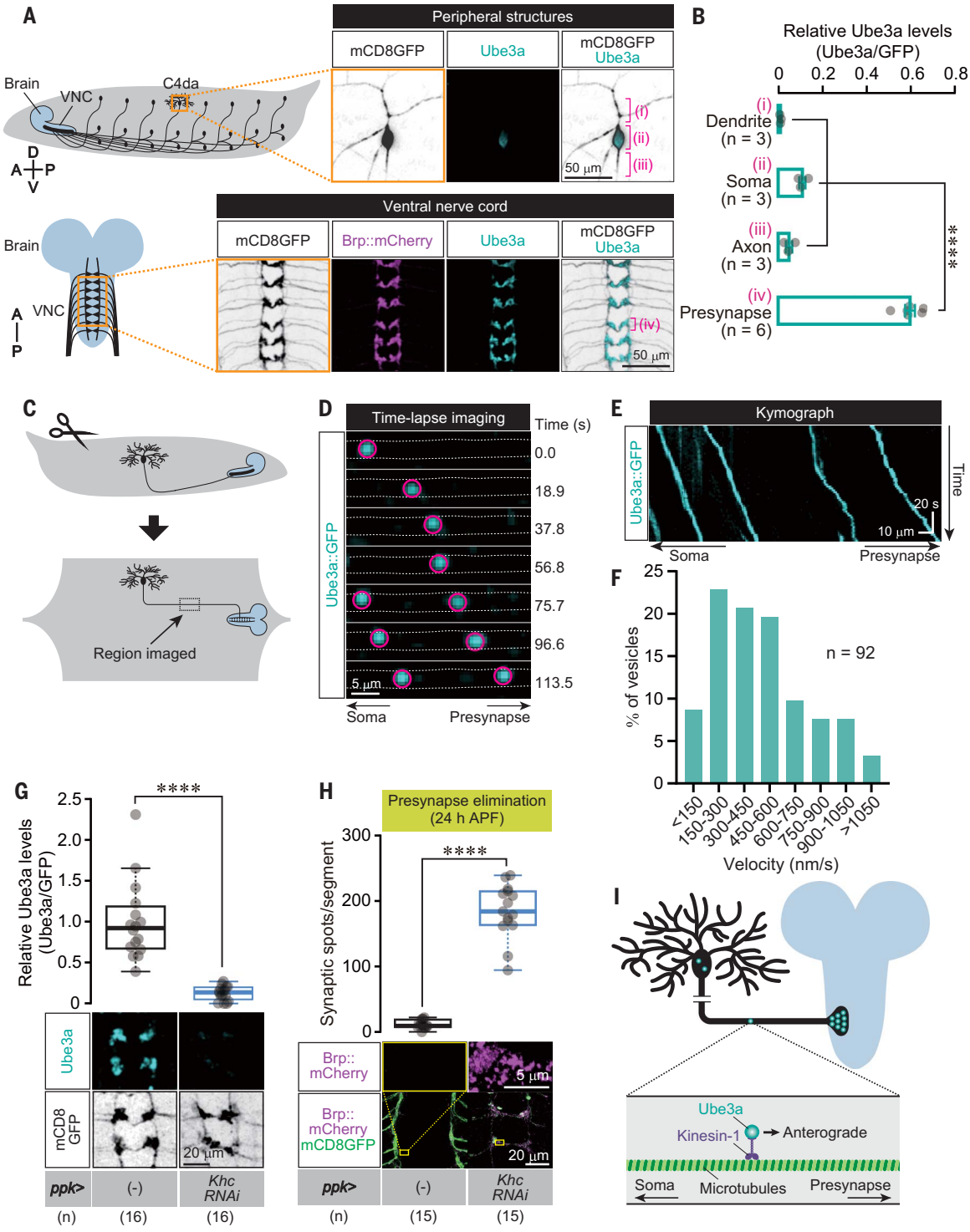

Fig. 3. Ube3a is transported to presynapses in a kinesin motor–dependent manner. (**A**) Subcellular locations of Ube3a-Flag (cyan) in peripheral compartments and the VNC in larval C4da neurons. (i), (ii), (iii), and (iv) indicate the regions of dendrites, soma, axons, and presynapses, respectively. (**B**) Relative expression levels of Ube3a-Flag in each subcellular compartment of C4da neurons. Data are shown as the mean ± SEM. ****$P < 0.0001$, one-way analysis of variance (ANOVA), followed by Tukey's multiple-comparisons test. (**C**) Schematic images of preparations for time-lapse imaging of Ube3a::GFP in C4da axons. (**D**) Time-lapse images showing anterograde transport of Ube3a::GFP vesicles (red circles) in C4da axons. (**E**) Representative kymographs of the anterograde transport of Ube3a::GFP-positive vesicles within C4da axons. (**F**) Velocity of anterograde transport of Ube3a::GFP-positive vesicles. (**G**) Relative expression levels of Ube3a-Flag in axon terminals of *khc*-suppressed neurons. Box plots indicate the median, 25th and 75th percentiles, the data range except for outliers, and outliers. ****$P < 0.0001$, Mann-Whitney test. (**H**) Presynapse numbers in an abdominal segment at 24 hours APF. Box plots indicate the median, 25th and 75th percentiles, and the data range. ****$P < 0.0001$, Mann-Whitney test. (**I**) A schematic image of axonal transport of Ube3a.

Downloaded from https://www.science.org at University Van Amsterdam on April 13, 2025

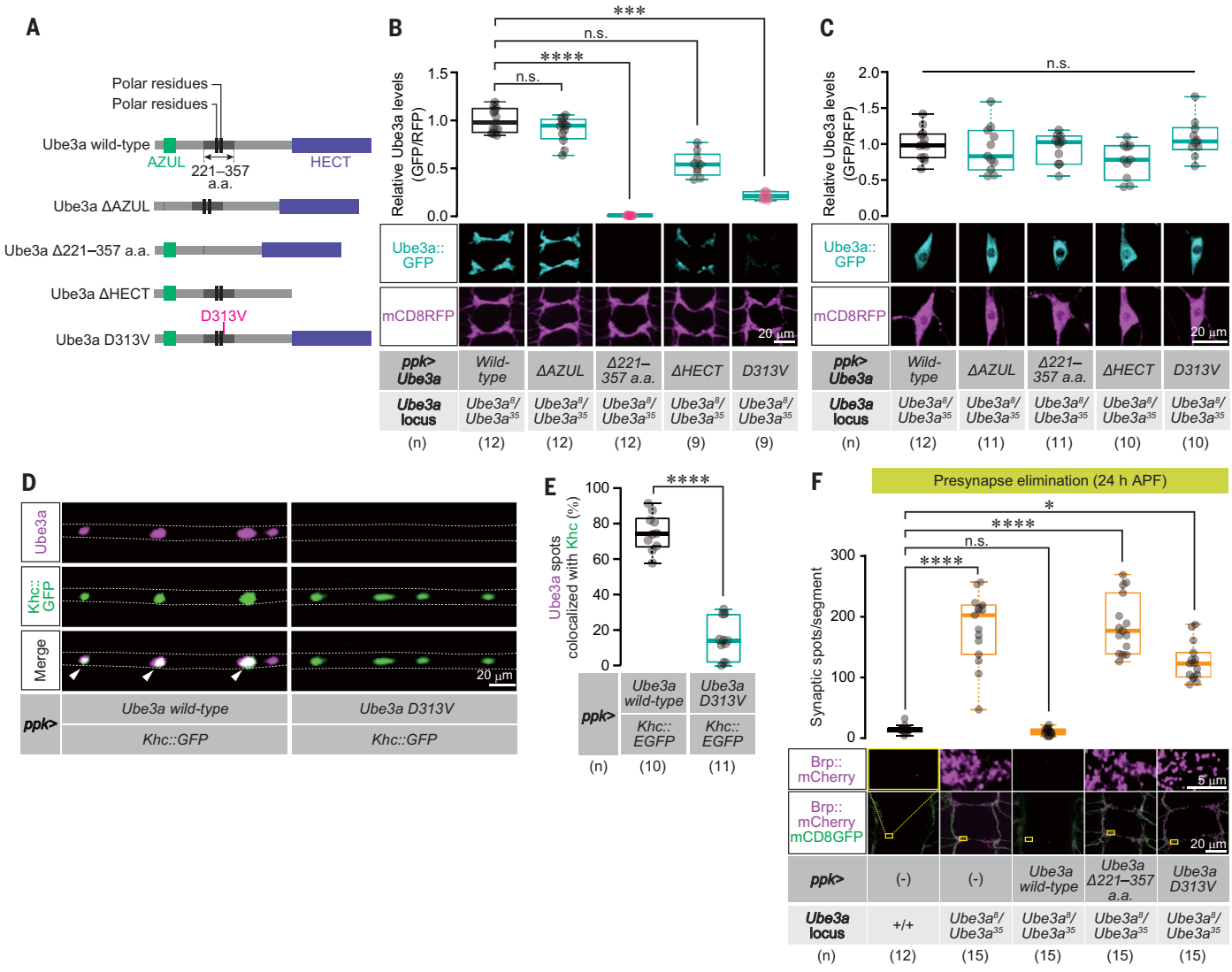

Fig. 4. Angelman syndrome–associated mutations attenuate axonal transport and presynapse localization of Ube3a. (**A**) Schematic views of wild-type and mutant Ube3a::GFP used in this study. (**B** and **C**) Relative expression levels of Ube3a::GFP with a domain deletion or an Angelman syndrome missense mutation in the (B) axon terminals and (C) soma. Box plots indicate the median, 25th and 75th percentiles, and the data range. ****$P < 0.0001$, ***$P < 0.001$, n.s. $P \geq 0.05$, Kruskal-Wallis test with Dunn's multiple comparisons test. (**D**) Colocalization of Ube3a-Flag (wild-type or D313V) and Khc::GFP in C4da axons. Arrowheads indicate Ube3a-Flag (magenta) and Khc::GFP (green)–double-positive vesicles. (**E**) Percentages of Ube3a-Flag (wild-type or D313V) and Khc::GFP–double-positive vesicles. Box plots indicate the median, 25th and 75th percentiles, and the data range. ****$P < 0.0001$, Mann-Whitney test. (**F**) Presynapse numbers in an abdominal segment. Box plots indicate the median, 25th and 75th percentiles, and the data range. ****$P < 0.0001$, *$P < 0.05$, n.s. $P \geq 0.05$, Kruskal-Wallis test with Dunn's multiple comparisons test.

Tkv in C4da neurons (Fig. 5A). No notable defect was observed in dendrite pruning by overexpressing a constitutive active version of Tkv in C4da neurons (fig. S10). We thus checked Tkv expression levels in C4da neurons using a Tkv::GFP reporter and found that presynaptic Tkv levels were significantly reduced by 8 hours APF (Fig. 5B), suggesting that BMP signaling is down-regulated in C4da neurons during early stages of metamorphosis. This Tkv reduction was significantly attenuated in *Ube3a*-null mutants (Fig. 5B), suggesting that Ube3a mediates Tkv down-regulation in C4da neurons. Given that BMP signaling induces Mad phosphorylation (*36*, *37*), we next examined phosphorylated Mad (pMad) levels in C4da neurons. Consistent with the Tkv levels (Fig. 5B), pMad levels in the C4da soma were significantly reduced by 8 hours APF in wild-type control, whereas the pMad reduction was significantly attenuated in *Ube3a*-null mutants (fig. S11). Removal of one copy of *tkv* or *mad*, both of which encode essential components of BMP signaling, largely rescued the presynapse elimination defects of *Ube3a*-null mutants at 24 hours APF (Fig. 5C), providing genetic evidence that enhanced BMP signaling is responsible for the presynapse elimination defects in *Ube3a*-null mutants. Consistent with this notion, synapse elimination defects in *Ube3a*-null mutants were ameliorated by feeding of the selective BMP antagonist LDN-193189 (Fig. 5D) and by expressing Glued-DN or Dad in C4da neurons; both are known to inhibit pMad signaling (fig. S12) (*38*, *39*). These data consistently indicate that Ube3a promotes synapse elimination in C4da neurons at least in part by down-regulating synaptic BMP signaling (Fig. 5E).

Downloaded from https://www.science.org at University Van Amsterdam on April 13, 2025

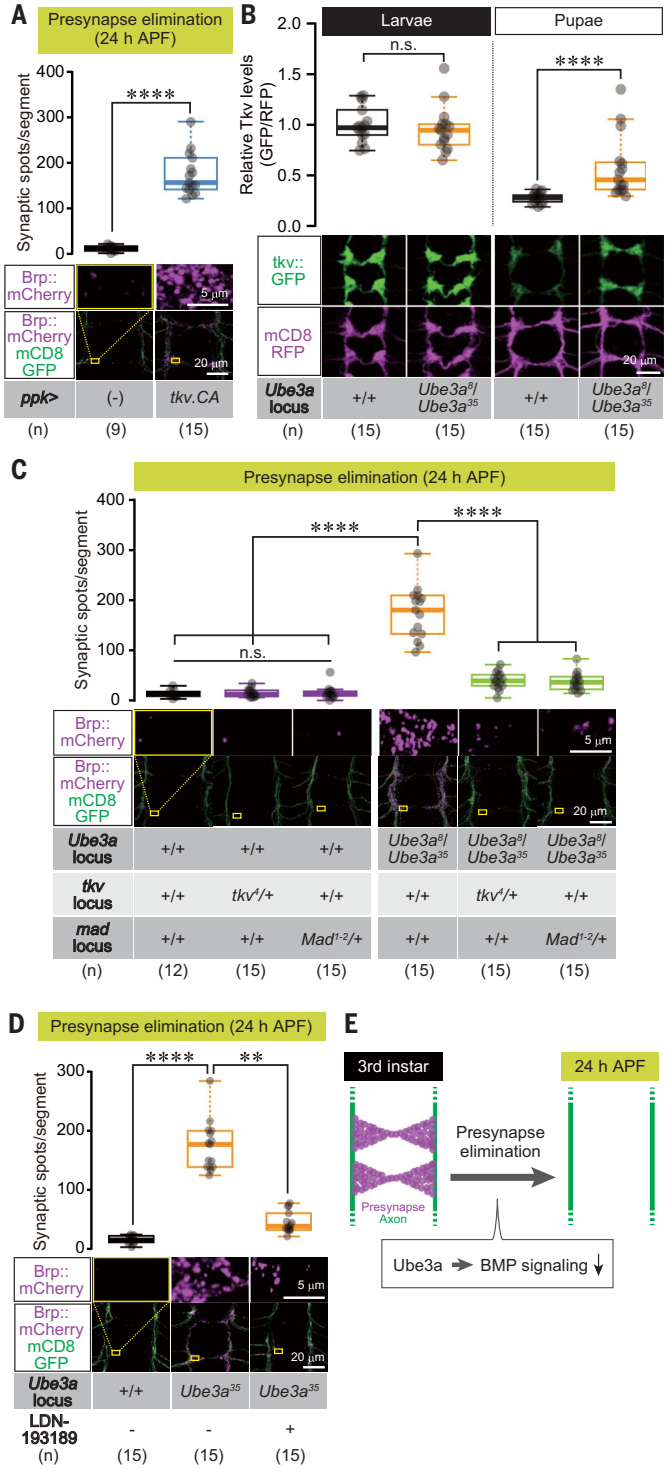

Fig. 5. Ube3a promotes synapse elimination through down-regulation of synaptic BMP signaling. (**A**) Presynaptic numbers in an abdominal segment of C4da neurons at 24 hours APF. Box plots indicate the median, 25th and 75th percentiles, and the data range. ****P < 0.0001, Mann-Whitney test. (**B**) (Top) Relative expression levels of Tkv::GFP at the third instar larval stage (larvae) or 8 hours APF (pupae) in wild-type and *ube3a*-null mutants. Box plots indicate the median, 25th and 75th percentiles, the data range except for outliers, and outliers. ****P < 0.0001, n.s. $P \geq 0.05$, Mann-Whitney test. (**C**) Presynaptic numbers in an abdominal segment of C4da neurons at 24 hours APF. Box plots indicate the median, 25th and 75th percentiles, the data range except for outliers, and outliers. ****P < 0.0001, n.s. $P \geq 0.05$, Kruskal–Wallis test with Dunn's multiple comparisons test. (**D**) Presynaptic numbers in an abdominal segment of C4da neurons at 24 hours APF. Box plots indicate the median, 25th and 75th percentiles, the data range except for outliers, and outliers. ****P < 0.0001, **P < 0.01, Kruskal-Wallis test with Dunn's multiple comparisons test. (**E**) Ube3a down-regulates presynaptic BMP signaling for presynapse elimination in C4da neurons.

Increased Ube3a activity in presynapses causes precocious synapse elimination and impairs synapse transmission

In addition to loss of Ube3a, increased Ube3a dosage is associated with ASDs (*2*, *7*), yet it remains unknown whether increased activity of presynaptic Ube3a might contribute to synapse dysfunction in vivo. To address this issue, we next overexpressed wild-type and mutant Ube3a in C4da neurons and found that overexpression of wild-type Ube3a caused severe presynapse loss in C4da axon terminals in all segments of the third instar larvae (Fig. 6A and figs. S2, C and D). Second instar larvae with Ube3a overexpression showed no obvious changes in the presynapse number compared with that of wild-type control (Fig. 6A), suggesting that increased Ube3a expression in C4da neurons causes precocious elimination of existing presynapses rather than reduction of synapse formation in the earlier larval stages. This precocious synapse elimination was undetectable by overexpressing a catalytically inactivated Ube3a mutant (C941A) or Ube3a harboring an Angelman syndrome mutation (D313V) in C4da neurons (Fig. 6A). In addition, the precocious synapse elimination was partially suppressed by overexpressing a constitutive active Tkv (fig. S13). These data together indicate that increased Ube3a E3 ligase activity in C4da presynapses promotes precocious synapse elimination by down-regulating BMP signaling. We next assessed whether increased Ube3a activity in presynapses might affect synaptic transmission as well as synapse number. To do that, in live larval preparations we optogenetically activated C4da neurons with Channelrhodopsin2 (ChR2) while monitoring intracellular calcium (Ca^{2+}) responses in the downstream A08n neurons expressing jRGEGO1a (Fig. 6B) (*24*, *40*). We found that the C4da-to-A08n synapse transmission upon optogenetic activation of C4da neurons was significantly reduced by overexpressing wild-type Ube3a, but not Ube3a (C941A) and Ube3a (D313V) mutants, in C4da neurons (Fig. 6, C to E). We further checked the impact of Ube3a overexpression on nociceptive behavior in larvae because C4da sensory neurons detect multiple noxious stimuli and evoke robust escape behavior (*24*, *25*, *40*, *41*). To this end, we tested larval rolling latencies using a temperature-controlled probe for local thermonociceptive stimulation (Fig. 6F) (*24*, *25*, *40*, *41*). Consistent with the reduced synapse number and transmission in C4da neurons, third instar larvae overexpressing wild-type Ube3a, but not the catalytically inactive Ube3a (C941A) and the Ube3a with the Angelman syndrome–associated mutation (D313V), showed significantly longer rolling latencies in response to noxious heat stimuli (Fig. 6G), indicating that increased Ube3a activity in presynapses of nociceptive neurons causes hypoalgesia. Hypoalgesia phenotypes are associated with certain types of ASD patients and ASD model mice (*42*–*44*). Taken together, these data all consistently indicate that increased Ube3a activity in presynapses affects synapse numbers and synapse transmission in vivo.

Discussion

In this study, we have established a presynaptic role of Ube3a in synapse elimination and revealed the molecular mechanism underlying presynaptic targeting of Ube3a proteins. We have further shown that Ube3a promotes presynapse elimination by suppressing presynaptic BMP signaling, which presumably causes instability and thus reduction of existing synapses. Last, we have shown that not only reduced activity but also increased activity of

Downloaded from https://www.science.org at University Van Amsterdam on April 13, 2025

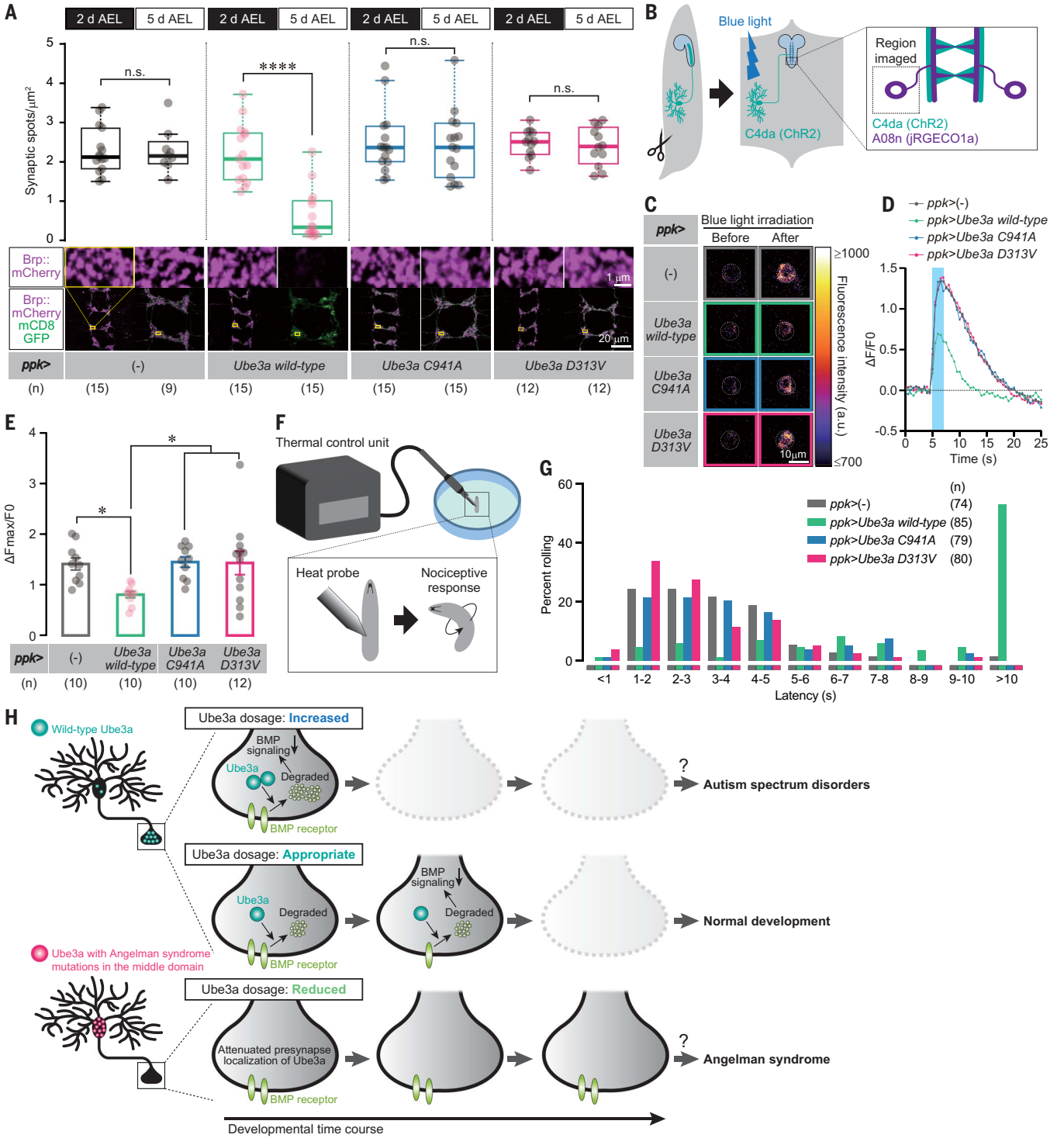

Fig. 6. Increased Ube3a activity in presynapses causes precocious synapse elimination and impairs synapse transmission. (**A**) Presynaptic numbers in an abdominal segment of C4da neurons at 2 days after egg laying (AEL) or 5 days AEL. Box plots indicate the median, 25th and 75th percentiles, the data, range except for outliers, and outliers. ****$P < 0.0001$, n.s. $P \geq 0.05$, Mann-Whitney test. (**B**) Schematic images of preparations for calcium imaging in A08n neurons upon C4da activation. (**C**) Ca^{2+} imaging of A08n neurons upon C4da activation. (**D**) Time series for the average of Ca^{2+} responses in A08n neurons upon optogenetic activation of C4da neurons overexpressing wild-type or mutant Ube3a at the third instar larval stage. (**E**) Average of A08n maximal fluorescence increase ($\Delta F_{max}/F_0$) values upon optogenetic activation of C4da neurons overexpressing wild-type or mutant Ube3a. Data are expressed as the mean ± SEM. *$P < 0.05$, one-way ANOVA, followed by Tukey's multiple-comparisons test. (**F**) Experimental setup for local hot probe assay. (**G**) Latency of nociceptive rolling responses in the third instar larvae overexpressing wild-type or mutant Ube3a. (**H**) Presynaptic Ube3a activity is associated with abnormalities of the synaptic structures and functions.

Downloaded from https://www.science.org at University Van Amsterdam on April 13, 2025

presynaptic Ube3a E3 ligase affect synaptic structure and function (Fig. 6H). These findings indicate that presynaptic Ube3a E3 ligase is a crucial factor to control synapse number and activity and suggest that mislocalization as well as dysregulation of Ube3a E3 activity might cause aberrant synapse function and neurodevelopmental disorder. In addition to the ecdysone-induced synapse elimination in C4da neurons, we found that presynaptic Ube3a is required for activity-dependent synapse elimination in *Drosophila* photoreceptor neurons (fig. S14, A and B) (*45*). Further genetic evidence suggests that, consistent with the ecdysone-induced synapse elimination in C4da neurons, Ube3a promotes activity-dependent synapse elimination through down-regulation of BMP signaling (fig. S14, C and B). These data support the notion that Ube3a and BMP down-regulation are required for activity-dependent synapse elimination as well as hormone-induced synapse elimination.

Angelman syndrome–associated missense mutations are distributed throughout the human Ube3a protein (figs. S7 and S8), and the pathological impact of each mutation, especially mutations localized between Azul and HECT domains, remains largely unknown. Our findings indicate that the Angelman syndrome–associated mutation D313V in the middle domain disrupts the presynaptic targeting and the function of Ube3a in synapse elimination. It will be intriguing to examine whether other Angelman syndrome–associated mutations might affect synaptic localization of Ube3a in neurons. Our data indicate that the middle domain of Ube3a plays a critical role for association of Ube3a with the kinesin-motor complex and thus presynaptic localization. Because Ube3a is localized in multiple neural compartments (*12*–*14*, *46*), it is of importance to define the compartment-specific role as well as substrates of Ube3a in neural development and function for comprehensive understanding the physiological and pathological role of Ube3a.

We propose that presynaptic Ube3a promotes Tkv down-regulation in C4da neurons. Previous reports suggest that the endocytic pathway controls BMP receptor levels in *Drosophila* neuromuscular junctions (NMJ) (*47*–*49*). We checked whether the endocytic pathway might contribute to Tkv down-regulation in C4da synapses and found that neither overexpression nor RNAi suppression of the components involved in the endocytic control of BMP receptors caused synapse eliminations defects in C4da neurons (fig. S15, A and B). Furthermore, neither overexpression nor RNAi suppression of the components affected reduction of Tkv levels in C4da presynapses during metamorphosis (fig. S16). It is thus likely that the Ube3a-mediated pathway, rather than the endocytic pathway, likely play a dominant role for Tkv down-regulation in C4da neurons during metamorphosis. In *Drosophila* NMJ, multiple molecular pathways, including actin regulation and hormone signaling, function downstream of or in parallel to BMP signaling for synapse development and remodeling (*38*, *39*, *50*, *51*). We checked the potential molecules and found that genetic manipulations of Ftz-f1/Hr39 attenuated both synapse elimination and dendrite pruning in C4da neurons (fig. S17). A previous work on axon pruning in mushroom body (MB) neurons indicated that Ftz-f1/Hr39 promotes axon pruning by up-regulating EcR-B1 levels in parallel to BMP signaling (*52*). Consistently, EcR-B1 levels were significantly reduced by Ftz-f1/Hr39 manipulations in C4da neurons (fig. S17). It is thus likely that Ftz-f1/Hr39 promotes both dendrite pruning and synapse elimination by up-regulating EcR-B1 levels in C4da neurons during metamorphosis. By contrast, presynaptic Ube3a and Tkv down-regulation are specifically required for synapse elimination but not for dendrite pruning, and *Ube3a* mutations and Tkv activation unaffected EcR-B1 levels in C4da neurons during metamorphosis (fig. S18). Therefore, similar to the case in *Drosophila* NMJ and MB neurons, Ftz-f1/Hr39 likely triggers global neural remodeling including dendrite pruning and synapse elimination through up-regulating EcR-B1 levels in C4da neurons, whereas presynaptic Ube3a and Tkv down-regulation locally promotes presynapse elimination at downstream of and/or in parallel to the Ftz-f1/Hr39/EcR signaling. Previous reports suggest that steroid hormones, such as estrogen and glucocorticoid, induce in the mammalian brain (*53*, *54*). It would be of interest to investigate whether presynaptic Ube3a and BMP down-regulation might play a role in steroid hormone–mediated synapse elimination in the mammalian brain.

In ASD model mice with chromosome 15q duplication, the synapse turnover is significantly enhanced because of accelerated synapse elimination and regeneration cycles, leading to synapse instability in cortical neurons (*55*). Given the augmented dosage of Ube3a in the Dup15q model mice, it is feasible that increased Ube3a activity in presynapses of ASD neurons might cause synapse instability and dysfunction. Consistent with this notion, increased dosage of Ube3a attenuates synaptic transmission in *Drosophila* neurons (Fig. 6) as well as mouse cortical neurons (*8*). Furthermore, a recent report indicates that presynaptic BMP signaling regulates synapse turnover in mouse cortical neurons (*56*). It is therefore likely that the role of Ube3a and BMP signaling in presynapses is conserved in flies and mammals. Given that pharmacological as well as genetic manipulations of BMP signaling suppressed synapse elimination defects through aberrant Ube3a functions, neuronal BMP signaling could be a target for interventions of ASD and Angelman syndrome. Further studies deciphering the presynaptic role of Ube3a and subsequent BMP signaling will provide insights into the regulation of local synapse elimination and neurodevelopmental pathology.

REFERENCES AND NOTES

1. K. Buiting, C. Williams, B. Horsthemke, *Nat. Rev. Neurol.* **12**, 584–593 (2016).
2. N. Khatri, H. Y. Man, *Front. Mol. Neurosci.* **12**, 109 (2019).
3. A. M. Mabb, M. C. Judson, M. J. Zylka, B. D. Philpot, *Trends Neurosci.* **34**, 293–303 (2011).
4. H. Kim, P. A. Kunz, R. Mooney, B. D. Philpot, S. L. Smith, *J. Neurosci.* **36**, 4888–4894 (2016).
5. M. Sato, M. P. Stryker, *Proc. Natl. Acad. Sci. U.S.A.* **107**, 5611–5616 (2010).
6. K. Yashiro *et al*., *Nat. Neurosci.* **12**, 777–783 (2009).
7. S. J. Lopez, D. J. Segal, J. M. LaSalle, *Front. Mol. Neurosci.* **11**, 476 (2019).
8. S. E. Smith *et al*., *Sci. Transl. Med.* **3**, 103ra97 (2011).
9. P. L. Greer *et al*., *Cell* **140**, 704–716 (2010).
10. S. S. Margolis *et al*., *Cell* **143**, 442–455 (2010).
11. J. Sun *et al*., *Cell Rep.* **12**, 449–461 (2015).
12. A. C. Burette *et al*., *J. Comp. Neurol.* **525**, 233–251 (2017).
13. A. C. Burette *et al*., *Mol. Autism* **9**, 54 (2018).
14. S. V. Dindot, B. A. Antalffy, M. B. Bhattacharjee, A. L. Beaudet, *Hum. Mol. Genet.* **17**, 111–118 (2008).
15. K. Emoto, *Curr. Opin. Neurobiol.* **22**, 805–811 (2012).
16. R. K. Morikawa, T. Kanamori, K. Yasunaga, K. Emoto, *Proc. Natl. Acad. Sci. U.S.A.* **108**, 19389–19394 (2011).
17. W. B. Grueber *et al*., *Development* **134**, 55–64 (2007).
18. T. Kanamori, K. Togashi, H. Koizumi, K. Emoto, *Int. Rev. Cell Mol. Biol.* **318**, 1–25 (2015b).
19. K. Furusawa, K. Emoto, *Front. Cell. Neurosci.* **14**, 613320 (2021).
20. Y. Kitatani *et al*., *PLOS Genet.* **16**, e1008942 (2020).
21. C. T. Kuo, L. Y. Jan, Y. N. Jan, *Proc. Natl. Acad. Sci. U.S.A.* **102**, 15230–15235 (2005).
22. D. W. Williams, J. W. Truman, *Development* **132**, 3631–3642 (2005).
23. W. Fouquet *et al*., *J. Cell Biol.* **186**, 129–145 (2009).
24. C. Hu *et al*., *Nat. Neurosci.* **20**, 1085–1095 (2017).
25. J. Yoshino, R. K. Morikawa, E. Hasegawa, K. Emoto, *Curr. Biol.* **27**, 2499–2504.e3 (2017).
26. D. Kirilly *et al*., *Neuron* **72**, 86–100 (2011).
27. T. Kanamori *et al*., *Science* **340**, 1475–1478 (2013).
28. T. Kanamori, J. Yoshino, K. Yasunaga, Y. Dairyo, K. Emoto, *Nat. Commun.* **6**, 6515 (2015).
29. C. T. Kuo, S. Zhu, S. Younger, L. Y. Jan, Y. N. Jan, *Neuron* **51**, 283–290 (2006).
30. D. W. Williams, S. Kondo, A. Krzyzanowska, Y. Hiromi, J. W. Truman, *Nat. Neurosci.* **9**, 1234–1236 (2006).
31. J. J. Wong *et al*., *PLOS Biol.* **11**, e1001657 (2013).
32. H. H. Lee, L. Y. Jan, Y. N. Jan, *Proc. Natl. Acad. Sci. U.S.A.* **106**, 6363–6368 (2009).
33. M. T. Kelliher *et al*., *J. Cell Biol.* **217**, 2531–2547 (2018).
34. G. L. Sell, S. S. Margolis, *Front. Neurosci.* **9**, 322 (2015).
35. W. Li *et al*., *PLOS Genet.* **12**, e1006062 (2016).
36. H. Keshishian, Y. S. Kim, *Trends Neurosci.* **27**, 143–147 (2004).
37. E. Eivers, H. Demagny, E. M. De Robertis, *Cytokine Growth Factor Rev.* **20**, 357–365 (2009).
38. H. Aberle *et al*., *Neuron* **33**, 545–558 (2002).
39. B. A. Eaton, G. W. Davis, *Neuron* **47**, 695–708 (2005).
40. T. Kaneko *et al*., *Neuron* **95**, 623–638.e4 (2017).
41. W. D. Tracey Jr., R. I. Wilson, G. Laurent, S. Benzer, *Cell* **113**, 261–273 (2003).
42. S. I. Deutsch, *Am. J. Ment. Defic.* **90**, 631–635 (1986).
43. D. J. Fairburn *et al*., *Behav. Brain Res.* **420**, 113727 (2022).
44. L. Wang *et al*., *Neuropharmacology* **111**, 323–334 (2016).
45. A. Sugie *et al*., *Neuron* **86**, 711–725 (2015).
46. R. Avagliano Trezza *et al*., *Nat. Neurosci.* **22**, 1235–1247 (2019).
47. X. Wang, W. R. Shaw, H. T. Tsang, E. Reid, C. J. O'Kane, *Nat. Neurosci.* **10**, 177–185 (2007).

Downloaded from https://www.science.org at University Van Amsterdam on April 13, 2025

48. K. M. O'Connor-Giles, L. L. Ho, B. Ganetzky, *Neuron* **58**, 507–518 (2008).
49. R. J. Gleason, A. M. Akintobi, B. D. Grant, R. W. Padgett, *Proc. Natl. Acad. Sci. U.S.A.* **111**, 2578–2583 (2014).
50. A. Boulanger, M. Farge, C. Ramanoudjame, K. Wharton, J. M. Dura, *PLOS ONE* **7**, e40255 (2012).
51. Z. D. Piccioli, J. T. Littleton, *J. Neurosci.* **34**, 4371–4381 (2014).
52. A. Boulanger *et al*., *Nat. Neurosci.* **14**, 37–44 (2011).
53. B. S. McEwen, *Front. Neuroendocrinol.* **49**, 8–30 (2018).
54. B. S. McEwen, *Brain Res.* **1645**, 50–54 (2016).
55. M. Isshiki *et al*., *Nat. Commun.* **5**, 4742 (2014).
56. T. Higashi, S. Tanaka, T. Iida, S. Okabe, *Cell Rep.* **22**, 919–929 (2018).

ACKNOWLEDGMENTS

We thank Y. Q. Zhang, C. Doe, T. Suzuki, and J. Parrish for valuable reagents; Bloomington stock center, Kyoto Stock Center, and Vienna Drosophila Resource Center for fly stocks; J. Parrish for critical reading and comments on the draft; H. Ito and M. Maetani for technical assistance; and the members of Emoto Lab for critical comments and discussion. **Funding:** This work is supported by MEXT Grants-in-Aid for Scientific Research on Innovative Areas "Dynamic regulation of brain function by Scrap and Build system" (KAKENHI 16H06456), JSPS (KAKENHI 16H02504), WPI-IRCN, AMED-CREST (JP21 g310010), JST-CREST (JPMJCR22P6), Toray Foundation, Naito Foundation, Takeda Science Foundation, and Uehara Memorial Foundation to K.E.; JSPS (KAKENHI 18J01378 and 21K15102) to K.F.; and The Leading Initiative for Excellent Young Researchers (LEADER) from MEXT and JSPS (KAKENHI 22K06309) and AMED-PRIME (JP22 g6510011) to K.I. **Author contributions:** Initiation and conceptualization: K.E. Investigation: K.F., K.I., M.T., N.T., and E.H. Writing - original draft: K.E. Writing - editing: K.F. and K.E., with inputs from all authors. Visualization: K.F., K.I., M.T., and K.E. Supervision: E.H. and E.K. Funding acquisition: K.F., K.I., and K.E. **Competing interests:** The authors declare no conflicts of interest. **Data and materials availability:** All data are available in the main text or the supplementary materials. **License information:** Copyright © 2023 the authors, some rights reserved; exclusive licensee American Association for the Advancement of Science. No claim to original US government works. https://www.science.org/about/science-licenses-journal-article-reuse

SUPPLEMENTARY MATERIALS

science.org/doi/10.1126/science.ade8978
Materials and Methods
Figs. S1 to S18
Tables S1 and S2
References (*57*–*62*)
Movies S1 to S4
MDAR Reproducibility Checklist

Submitted 15 September 2022; resubmitted 6 June 2023
Accepted 18 August 2023
10.1126/science.ade8978

Downloaded from https://www.science.org at University Van Amsterdam on April 13, 2025